

Deformable Registration Framework for Augmented Reality-based Surgical Guidance in Head and Neck Tumor Resection

Qingyun Yang^{1*}[0009-0001-8283-2892], Fangjie Li^{1*}[0009-0008-6628-812X], Jiayi Xu¹[0009-0006-6108-1117], Zixuan Liu¹[0009-0007-2618-2147], Sindhura Sridhar²[0009-0009-3649-3920], Whitney Jin²[0009-0002-1415-0723], Jennifer Du³[0009-0004-8534-3703], Jon Heiselman¹[0000-0002-4414-8846], Michael Miga¹[0000-0002-0694-9765], Michael Topf^{1,2}[0000-0002-1022-4417], and Jie Ying Wu¹[0000-0002-7306-8140]

¹ Vanderbilt University, Nashville TN 37235, USA
JieYing.Wu@vanderbilt.edu

² Vanderbilt University Medical Center, Nashville TN 37232, USA

³ Vanderbilt University School of Medicine, Nashville TN 37240, USA

Abstract. Head and neck squamous cell carcinoma (HNSCC) has one of the highest rates of recurrence cases among solid malignancies. Recurrence rates can be reduced by improving positive margins localization. Frozen section analysis (FSA) of resected specimens is the gold standard for intraoperative margin assessment. However, because of the complex 3D anatomy and the significant shrinkage of resected specimens, accurate margin relocation from specimen back onto the resection site based on FSA results remains challenging. We propose a novel deformable registration framework that uses both the pre-resection upper surface and the post-resection site of the specimen to incorporate thickness information into the registration process. The proposed method significantly improves target registration error (TRE), demonstrating enhanced adaptability to thicker specimens. In tongue specimens, the proposed framework improved TRE by up to 33% as compared to prior deformable registration. Notably, tongue specimens exhibit complex 3D anatomies and hold the highest clinical significance compared to other head and neck specimens from the buccal and skin. We analyzed distinct deformation behaviors in different specimens, highlighting the need for tailored deformation strategies. To further aid intraoperative visualization, we also integrated this framework with an augmented reality-based auto-alignment system. The combined system can accurately and automatically overlay the deformed 3D specimen mesh with positive margin annotation onto the resection site. With a pilot study of the AR guided framework involving two surgeons, the integrated system improved the surgeons' average target relocation error from 9.8 cm to 4.8 cm.

Keywords: Deformable Registration · Head and Neck Cancer · Soft-tissue Deformation.

* These authors contributed equally to this work

1 Introduction

Approximately 890,000 new cases of head and neck squamous cell carcinoma (HNSCC) are diagnosed worldwide each year [1]. HNSCC has one of the highest positive margin rates among solid cancers, leading to increased local recurrence, reduced survival, and higher treatment costs [7]. During tumor resections, intraoperative frozen section analysis is used to assess margin status, and if positive margins are detected, additional resection is performed. Thus, precise relocation of positive margins from histopathological analysis onto the patient is critical for effective re-resection. However, this process is particularly challenging in HNSCC. The k region’s complex 3D anatomy a3D variable specimen shrinkage further complicates accurate relocation. For this reason, only 29% of re-resections following an initial positive margin contain additional cancer [9].

To address this unmet need for increased guidance in relocating a positive margin, we have developed a protocol to create a 3D model of the resected cancer specimen using 3D scanning [8] which can be annotated with histopathological findings intraoperatively. We have leveraged our 3D specimen scanning protocol to provide additional visual guidance for surgeons through augmented reality (AR) 3D specimen holograms. However, a major challenge of this protocol is that surgical specimens deform during excision. Mucosal shrinkage (11.3 – 47.6%) following oral cavity resection has been documented in prior studies [13,5,6,2]. The deformation pattern could impact the ability of the surgeon to place a 3D specimen hologram back into the surgical defect locate the site of a positive margin. In our prior work [14], we used the 3D scan of the post-resection site (resection cavity after tissue removal) to guide the deformation. However, a single surface scan does not provide adequate constraints, especially for specimens with complex, non-planar shapes and varied thickness, such as tongue specimens.

There are three important tissue types in the head and neck area: skin, tongue, and buccal. Their deformation patterns are distinguished by two key features: tissue types and anatomical complexity. Both tongue and buccal specimens are oral tissues that undergo significant mucosal shrinkage post-resection. Structurally, the tongue exhibits a more complex 3D anatomical shape compared to buccal and skin specimens. Specifically, tongue specimens are significantly thicker and have a pre-resection surface that curves upward from the resection site. In contrast, buccal and skin specimens are relatively thin, with pre-resection surfaces that are nearly parallel to the underlying cavity. The tongue poses the greatest clinical challenge in margin relocalization due to its intricate structure.

In this work, we propose a new deformable registration framework for head and neck tissue. This framework introduces the pre-resection surface of the resection site as an additional constraint to deformable registration, in addition to the post-resection site. On cadaver specimens, the proposed framework achieved significantly lower target registration error (TRE) than both rigid and rigid registration with scaling (similarity registration).

We further demonstrated the clinical significance of the deformation framework by integration with an augmented reality head mounted display (AR-HMD) guidance system to visualize the deformed mesh on the patient resection cav-

ity. AR based guidance has shown promising results to guide head and neck surgery [9]. However, prior methods [12,10] did not use deformed meshes, and required manual positioning and alignment of the specimen mesh onto the resection cavity, limiting their effectiveness as an accurate guidance tool. To the best of our knowledge, we propose the first system for head and neck surgery with integrated deformable registration and AR guidance.

2 Methods

The proposed deformable registration and AR guidance framework is outlined in Fig. 1, and contrasted with the current standard of care, which is verbal guidance. The proposed method would provide visual guidance on the positive margin relocation task, which could be more intuitive than verbal guidance.

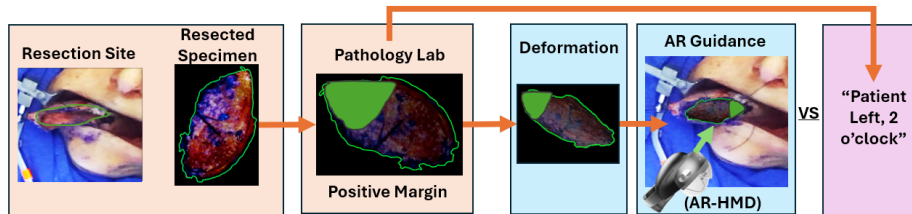


Fig. 1. The standard of care and proposed tumor resection workflows. In the standard of care, the surgeon relies purely on verbal instructions to locate the positive margin, leading to imprecise re-resection. AR guidance with deformable registration provides additional visual guidance.

2.1 Proposed Deformable Registration Framework

Problem Formulation In the deformable registration task for head and neck tumor resection, we have a 3D mesh of the resected tumor specimen, which has undergone shrinkage, and a point cloud describing the resection site. We also include corresponding fiducials on the specimen and the resection site. In deformable registration, we aim to deform the specimen such that it can map to the resection site, as illustrated in 2. The fiducials, which have one-to-one correspondence, are used to guide the deformation process.

Input Data Fig. 2 shows the data that is available for the deformable registration task.

1. Intraoperatively textured point clouds of the pre-resection surface of the surgical site, and post-resection site, V_{surf}^{pc} and V_{cav}^{pc} , shown in Fig. 2a.

2. Dense 3D mesh of the resected specimen, M^{spec} .
3. Four corresponding fiducial landmarks present on both the resection site (V_{srf}^{fids} , V_{cav}^{fids}) and the specimens V_{spec}^{fids} . These landmarks allow us to perform a rigid point-set alignment between the resection site and the specimen. They are also used in the deformation algorithm outlined below.

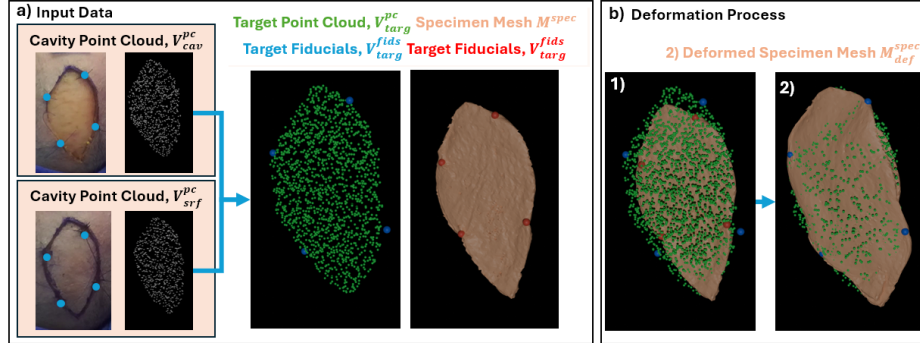


Fig. 2. a) A range of input data of the deformation registration task. b) The expected output of the deformation task.

We then combine V_{srf}^{pc} and V_{cav}^{pc} to produce the target point cloud, V_{targ}^{pc} . This is achieved through a rigid alignment between the two scans, using fiducial markers, V_{srf}^{fids} and V_{cav}^{fids} . We use V_{targ}^{pc} as deformation target, instead of only V_{cav}^{pc} , as in the prior method. As mentioned, the additional surface data would act as additional constraint that would better guide the deformation process.

Deformable Registration Algorithm We use a Kelvinlet-based deformable registration [11]. To avoid unrealistic deformations, we incorporate strain energy based regularization to the optimization goal. An isotropic scaling factor is also incorporated, following the approach from [4], to correct for uniform tissue shrinkage. For the Kelvinlet model, we used $k = 45$ control points, a radial scale parameter of 0.01 m, a strain energy regularization weight of $10^{-11} Pa^{-2}$, a Poisson's ratio of 0.45 and Young's modulus of 2100 Pa. To facilitate visual guidance, we employed the HoloLens 2 (Microsoft, Seattle, WA) HMD to superimpose a rendered overlay of the deformed specimen onto the resection site. The AR interface is developed using Unity 3D (Unit3D2019), relying on the Microsoft Mixed Reality Toolkit (MRTK).

Automatic Registration The process to overlay the specimen mesh onto the resection cavity is detailed Fig. 3. An ArUco marker [3] is affixed to the surface of the cadaver head prior to resection. Following resection, the post-resection point cloud V_{cav}^{pc} is acquired, and the poses of both the ArUco marker and the

resection site are identified. Using these poses, the deformed mesh was registered to the ArUco marker and subsequently uploaded to the HMD. The HMD continuously tracks the ArUco marker on the cadaver surface, allowing for the virtual, annotated mesh to be overlaid onto the resection cavity, enabling visual guidance.

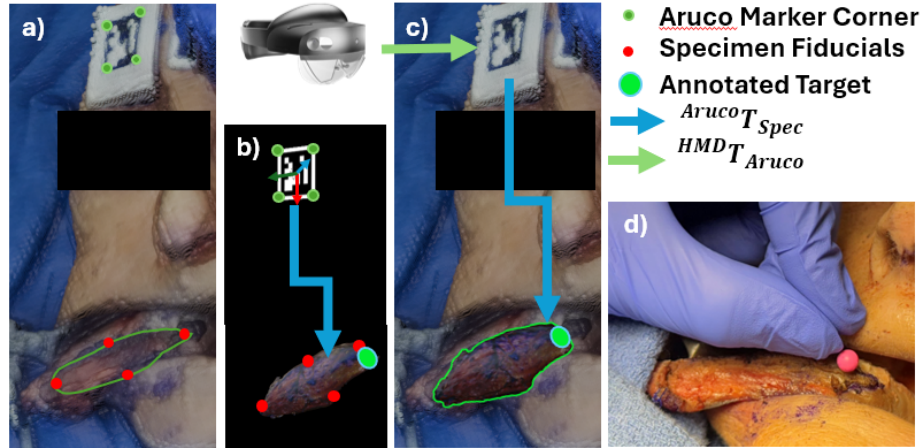


Fig. 3. General Workflow of the AR system. a) From 3D scan of the post-resection site, we obtain the pose of the resection site and of the ArUco marker. b) We then compute the transformation between the ArUco marker and the resection site c) The surgeon wearing the HMD can visualize the annotated specimen mesh, automatically overlaid on the surgical site. d) For our end-to-end evaluation task, the surgeon is asked to place a surgical pin on the target.

3 Experiment Setup and Data Collection

Data Acquisition for Deformable Registration We obtain 3 fresh frozen cadaver heads which has similar tissue properties to live tissue. A head and neck cancer surgeon, who performs approximately 50 locally advanced head and neck surgical resections annually, resected specimens similar to clinical cases. Before resections, he used an ink pen to mark the surgical plan. He added 4 pairs of sutured stitches at the corresponding locations on the boundaries of both the specimen and the resection site.

We used a structured light 3D scanner (EinScan SP, Shining 3D, Hangzhou, China) to generate a 3D, textured mesh of the resected specimen [8]. We used an RGBD camera (ZED 2i stereo camera, Stereolabs Inc., San Francisco, CA, USA), to capture sparse colored point clouds of the resection site, pre- and post-resection. We attached the camera to a mechanical arm, allowing the camera to operate overhead, without interfering with the surgeons. We manually segment

the pre-resection cavity and post-resection cavity from the full camera view. We manually label the fiducial points on the mesh and the point cloud. An example result is visible in Fig. 2a).

Deformable Registration Evaluation To evaluate the deformable registration, we measured TRE with cross validation. For each fold, we treat one fiducial as the target and exclude it from the registration. We then evaluate the mismatch between that fiducial’s estimated location through registration and the ground truth on the resection site point cloud. As comparison baselines, we used rigid registration and similarity registration (rigid registration with scaling) on the same combination of fiducials to perform TRE evaluation with paired T-test.

End-to-End Evaluation In order to evaluate the full surgical guidance system with deformable registration and AR, we designed an end-to-end evaluation study. For two specimens (one skin, one tongue), we randomly selected a fiducial as the target, and excluded it from the registration procedure as above. We asked the surgeon to remove all sutured fiducials from the resection site. To keep note of the ground truth target position, medical students were asked to record the ground truth position relative to salient anatomical landmarks.

Two surgeons relocated the target on the resection site. For each target, they first performed task with only verbal guidance. Then, they repeated the task with AR guidance. We measured the euclidean distance between their identified position and the ground truth. Prior to resection, the surgeons had access to the 3D scanned mesh specimen with annotated target.

4 Results

Deformable registration framework Fig. 4 shows that both deformable registration methods achieved significantly lower TRE than rigid and similarity registration ($p \leq 0.05$) averaged across all specimens. In 2 cases, similarity registration yielded a lower TRE (Table 1). However, similarity registration exhibited high variability and was not significantly more accurate than rigid registration ($p > 0.05$), except for skin specimens. Statistical testing did not demonstrate a significant difference between the two deformable registration methods. However, the maximum TRE is lower for our proposed method.

Across all three tongue cases, the proposed approach consistently achieved at least 20% lower TRE than the prior deformable method. Conversely, for buccal specimens, the prior deformable method consistently achieved lower TRE across all three cases. Notably, the proposed method did not improve performance compared to rigid registration in this category. For skin specimens, the advantage of the proposed method was less consistent, outperforming the prior method in 2 out of 3 cases. Table 2 shows that surgeons generally performed better with the AR guidance.

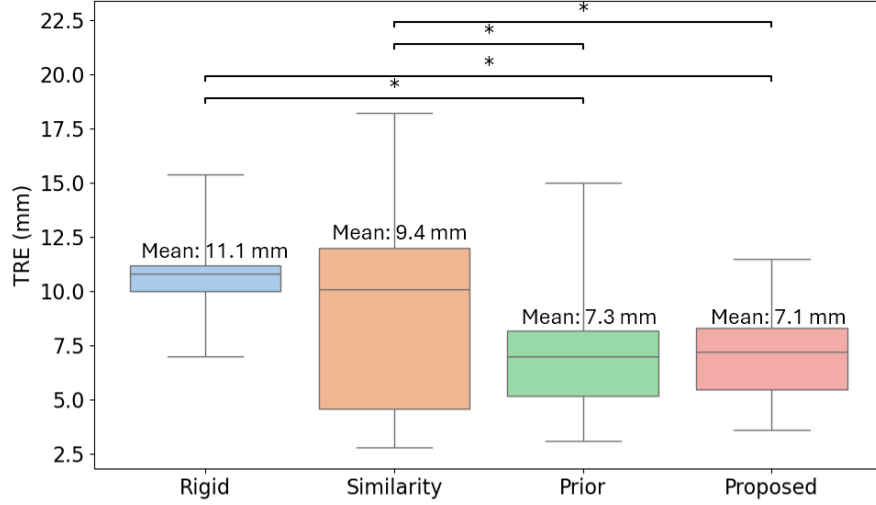


Fig. 4. The overall TRE (mm) of four different registration methods. The proposed method significantly outperforms the rigid and similarity registrations, which was not possible with the previous method. *: $p < 0.05$.

Table 1. TRE (mm) of all specimens, grouped by anatomical source.

Specimen	Rigid	Similarity	Prior method from [14]	Proposed
Tongue-1	15.4 ± 2.4	18.2 ± 2.6	15.0 ± 5.9	11.5 ± 3.1
Tongue-2	9.2 ± 4.6	3.7 ± 1.9	5.4 ± 2.3	4.3 ± 1.2
Tongue-3	14.9 ± 7.4	12.0 ± 1.0	8.2 ± 3.2	5.5 ± 5.1
Buccal-1	10.5 ± 6.0	13.6 ± 3.9	8.2 ± 4.4	8.7 ± 3.7
Buccal-2	7.0 ± 3.1	2.8 ± 0.9	4.9 ± 1.0	7.2 ± 1.5
Buccal-3	11.0 ± 1.7	8.7 ± 3.1	3.1 ± 1.2	7.2 ± 3.3
Skin-1	10.0 ± 1.1	4.6 ± 1.4	7.0 ± 0.9	3.6 ± 1.5
Skin-2	10.8 ± 3.8	10.1 ± 1.7	5.2 ± 3.2	7.2 ± 5.0
Skin-3	11.2 ± 1.5	10.9 ± 2.3	8.4 ± 4.2	8.3 ± 1.9

Table 2. TRE (mm) of two surgeons on two specimens

Guidance Type	Skin-1, User 1	Skin-1, User 2	Tongue-2, User 1	Tongue-2, User 2
Verbal	10	7.4	13	8.7
AR	6.1	3.4	1.0	8.7

5 Discussion

The proposed deformable registration outperformed the prior method in all tongue cases. The observed reduction in TRE indicates that incorporating the upper surface provides a meaningful constraint for guiding the registration process in tongue specimens, improving deformation accuracy. In contrast, for buccal specimens, the prior deformable registration performed best. Buccal specimens are thinner and have parallel upper and resection site surfaces. As a result, the additional constraint that incorporates thickness information may not be as beneficial and instead contributes to inconsistent deformation. Furthermore, buccal specimens are mucosal tissues that undergo significant shrinkage, exacerbating the discrepancy between the pre-resection surface and the resection site surface. A key challenge arises from the mismatch in deformation states: the upper surface data correspond to the pre-resection state, while the resection site point cloud represents the post-resection state. Registering the specimen mesh across these two different deformation states may introduce inconsistencies, ultimately leading to an unrealistic overall registration target. This pronounced difference in deformation states likely introduces inconsistencies in the registration process. However, given the limited data constraints available, incorporating additional information from the pre-resection specimen surface may nonetheless improve the registration result despite the change in surgical state.

Although skin specimens share a similar anatomical structure with buccal specimens, the proposed deformable registration outperformed the prior method in 2 out of 3 skin cases. Unlike oral specimens, which experience non-uniform mucosal shrinkage, skin specimens undergo more uniform shrinkage. This is supported by the finding that similarity-based registration consistently improved TRE across all three skin cases compared to rigid registration. Because skin specimens exhibit more consistent deformation states between the pre-resection surface and the resection site, incorporating additional surface information during registration led to improvement in TRE.

One limitation to our method is that we do not account for the deformation between the pre- and post-resection surfaces. One limitation of our experimental setup is that, data collection poses challenges, particularly for thinner specimens. The RGB-D camera cannot accurately capture the thickness information between the pre- and post-resection surfaces for buccal and skin specimens. This limitation reduces the reliability of the thickness constraint in guiding the proposed deformable registration. Lastly, we only have access to a limited number of cadaver specimens, limiting the strength of our deformation results. Nonetheless, our study is able to detect a significant improvement in TRE between rigid and nonrigid registration methods for relocalizing the margins of surgical specimens, with a substantial effect size that outweighs the predefined limits on the statistical power of our study.

These limitations highlight the challenges of registering specimens with complex deformation behaviors and underscore the need for further research to refine data acquisition methods and improve deformation consistency in registration.

6 Acknowledgement

This work was supported in part by the National Institute of Biomedical Imaging and Bioengineering of the National Institutes of Health through Grant R01EB027498, a National Cancer Institute (NCI) K08 Career Development Award - 1K08CA293255-0, Vanderbilt University Seeding Success Grant, and the VISE Physician-in-Residence program.

References

1. Barsouk, A., Aluru, J.S., Rawla, P., Saginala, K., Barsouk, A.: Epidemiology, Risk Factors, and Prevention of Head and Neck Squamous Cell Carcinoma. *Medical Sciences* **11**(2), 42 (6 2023). <https://doi.org/10.3390/medsci11020042>
2. El-Fol, H.A., Noman, S.A., Beheiri, M.G., Khalil, A.M., Kamel, M.M.: Significance of post-resection tissue shrinkage on surgical margins of oral squamous cell carcinoma. *Journal of Cranio-Maxillofacial Surgery* **43**(4), 475–482 (5 2015). <https://doi.org/10.1016/j.jcms.2015.01.009>
3. Garrido-Jurado, S., Muñoz-Salinas, R., Madrid-Cuevas, F.J., Marín-Jiménez, M.J.: Automatic generation and detection of highly reliable fiducial markers under occlusion. *Pattern Recognition* **47**(6), 2280–2292 (6 2014). <https://doi.org/10.1016/j.patcog.2014.01.005>
4. Heiselman, J.S., Richey, W.L., Taylor, S.L., Miga, M.I.: Improving accuracy of image-to-physical laparoscopic liver registration via reconstruction of intrahepatic pressure changes from abdominal insufflation. In: *Medical Imaging 2021: Image-Guided Procedures, Robotic Interventions, and Modeling*. vol. 11598, pp. 231–238. SPIE (2021)
5. Johnson, R.E., Sigman, J.D., Funk, G.F., Robinson, R.A., Hoffman, H.T.: Quantification of surgical margin shrinkage in the oral cavity. *Head & Neck: Journal for the Sciences and Specialties of the Head and Neck* **19**(4), 281–286 (1997)
6. Mistry, R.C., Qureshi, S.S., Kumaran, C.: Post-resection mucosal margin shrinkage in oral cancer: Quantification and significance. *Journal of Surgical Oncology* **91**(2), 131–133 (8 2005). <https://doi.org/10.1002/jso.20285>
7. Orosco, R.K., Tapia, V.J., Califano, J.A., Clary, B., Cohen, E.E., Kane, C., Lippman, S.M., Messer, K., Molinolo, A., Murphy, J.D., Pang, J., Sacco, A., Tringale, K.R., Wallace, A., Nguyen, Q.T.: Positive Surgical Margins in the 10 Most Common Solid Cancers. *Scientific Reports* **8**(1) (12 2018). <https://doi.org/10.1038/s41598-018-23403-5>
8. Perez, A.N., Sharif, K.F., Guelfi, E., Li, S., Miller, A., Prasad, K., Sinard, R.J., Lewis, J.S., Topf, M.C.: Ex vivo 3D scanning and specimen mapping in anatomic pathology. *Journal of Pathology Informatics* **14** (1 2023). <https://doi.org/10.1016/j.jpi.2022.100186>
9. Prasad, K., Fassler, C., Miller, A., Aweeda, M., Pruthi, S., Fusco, J.C., Daniel, B., Miga, M., Wu, J.Y., Topf, M.C.: More than meets the eye: Augmented reality in surgical oncology. *Journal of Surgical Oncology* **130**(3), 405–418 (2024). <https://doi.org/https://doi.org/10.1002/jso.27790>, <https://onlinelibrary.wiley.com/doi/abs/10.1002/jso.27790>
10. Prasad, K., Miller, A., Sharif, K., Colazo, J.M., Ye, W., Necker, F., Baik, F., Lewis, J.S., Rosenthal, E., Wu, J.Y., Topf, M.C.: Augmented-Reality Surgery to

- Guide Head and Neck Cancer Re-resection: A Feasibility and Accuracy Study. *Annals of Surgical Oncology* **30**(8), 4994–5000 (8 2023). <https://doi.org/10.1245/s10434-023-13532-1>
11. Ringel, M., Heiselman, J., Richey, W., Meszoely, I., Miga, M.: Regularized kelvinlet functions to model linear elasticity for image-to-physical registration of the breast. In: *International Conference on Medical Image Computing and Computer-Assisted Intervention*. pp. 344–353. Springer (2023)
 12. Tong, G., Xu, J., Pfister, M., Atoum, J., Prasad, K., Miller, A., Topf, M., Wu, J.Y.: Development of an augmented reality guidance system for head and neck cancer resection. *Healthcare Technology Letters* **11**(2-3), 93–100 (4 2024). <https://doi.org/10.1049/htl2.12062>
 13. Umstattd, L.A., Mills, J.C., Critchlow, W.A., Renner, G.J., Zitsch, R.P.: Shrinkage in oral squamous cell carcinoma: An analysis of tumor and margin measurements in vivo, post-resection, and post-formalin fixation. *American Journal of Otolaryngology - Head and Neck Medicine and Surgery* **38**(6), 660–662 (11 2017). <https://doi.org/10.1016/j.amjoto.2017.08.011>
 14. Yang, Q., Acar, A., Ringel, M.J., Heiselman, J.S., Miga, M.I., Topf, M., Wu, J.Y.: Nonrigid alignment of en bloc tissue specimen to resection bed to enhance correspondence for re-resection guidance. In: *Medical imaging 2025: image-guided procedures, robotic interventions, and modeling*. SPIE (2025)